Gradient-based Iterative Identification Method for Non-uniformly Sampled Input-nonlinear Systems

First Xiyuan Zou*. Second Li Xie. Third Ruilin Bai***. Fourth Huizhong Yang******

** School of Internet of Things Engineering, Jiangnan University, Wuxi,PR China, (e-mail: ws zxy@outlook.com).*

*** School of Internet of Things Engineering, Jiangnan University, Wuxi, PR China, (e-mail: xieli@jiangnan.edu.cn)*

**** School of Internet of Things Engineering, Jiangnan University, Wuxi, PR China, (e-mail: bairuilin@hotmail.com)*

***** School of Internet of Things Engineering, Jiangnan University, Wuxi, PR China, (e-mail: yhz@jiangnan.edu.cn)*

Abstract: This paper proposes an identification method of an input-nonlinear system with saturation and dead-zone nonlinearity using the asynchronous input-output data spaced by non-uniform intervals. The piecewise expression of the nonlinear part is simplified as an analytic function with an available switching function. By extending the traditional continuous linear time-invariant processes to non-uniformly sampled input-nonlinear systems, a concise input-output representation model is derived. Based on the key term separation principle and the auxiliary model identification idea, a gradient-based iterative identification algorithm is developed for simultaneously estimating all parameters of the derived model. Through a numerical example, the proposed algorithm shows its superior estimation accuracy compared to the auxiliary model-based forgetting factor stochastic gradient algorithm. Finally, the application to a two-tank system indicates the effectiveness of the proposed method.

Keywords: input-nonlinear system; Hammerstein system; iterative identification; non-uniform sampling; parameter estimation.

1. INTRODUCTION

Due to nonlinear devices and complex mechanisms, nonlinearities are commonly encountered in practical processes such as control systems (Na et al., 2017; Amer et al., 2021), satellite dynamics and chemical and biological processes. Nonlinear systems can be described by block- oriented nonlinear models, including Hammerstein models (Ding et al., 2013; Ding, 2013), Wiener models (Atitallah et al., 2020), Wiener-Hammerstein models (Paduart et al., 2012), and Hammerstein-Wiener models (Schoukens and Tiels, 2017). Hammerstein models refer to the systems composed of a static nonlinear part followed by a linear time-invariant part, which have been employed to describe a class of nonlinear systems with nonlinear input, such as quantization (Xing et al., 2015), hysteresis (Gao et al., 2015), and backlash (Giri et al., 2011). The saturation and dead-zone characteristic is a typical input nonlinearity in engineering practice and widely exists in actuators (Hu et al., 2008), for example, in piezoelectric translators, elec- tric servomotors (Tahoun, 2017), and surface ships (Xia et al., 2013). The existence of the nonlinearity can worsen system performance and even threaten system instability, which tends to bring about severe damage in industryapplication. Consequently, the research on its analysis, stability and controlling has received extensive attention (Oh and Park, 2000; Dong, 2015). The identification of saturation and dead-zone is of significant interest for further research on it.

Parameter estimation of Hammerstein systems is essential for in-depth analysis and study of linear systems (Pan et al., 2018) and nonlinear systems (Avila et al., 2017). There have been many identification methods proposed for Hammerstein systems with single rate (Pu et al., 2021; Zhang et al., 2017). Liu and Bai presented three iterative algorithms to estimate Hammerstein systems with three kinds of nonlinear blocks, infinite impulse response, the saturation and preload (Liu and Bai, 2007). To handle Hammerstein systems with colored noise, a stochastic algorithm was proposed by combining the maximum likelihood estimate with the key-term separation principle in (Li and Ding, 2011). Chen et al. used a gradient algorithm to identify the Hammerstein systems with continuous non- linearity (Chen et al., 2012), which only considered the single rate sampling.

There have been factors like data acquisition and transmission, frequency characteristics and hardware constraints, which can cause that the inputs and outputs are asynchronously measured with non-uniform sampling intervals.

There exists some work on the non-uniformly sampled- data systems, e.g., the related problems including modeling and estimation have been suggested in (Ding et al., 2009). The work analyzed the controllability and observability of the non-uniformly sampled systems and dis- cussed the method for reconstructing continuous systems from non-uniformly sampled discrete-time data. With a high dimensional parameter vector, the decomposition was used to obtain a set of submodels to be identified and a hierarchical identification algorithm with low computation was proposed (Liu et al., 2012). (Xu, 2017) estimated the parameters of transfer functions and (Xu et al., 2018) studied the parameter estimation problem of signal modeling. The widely employed approach to identifying non-uniformly sampled Hammerstein systems is the lifting technique (Ding and Lin, 2014; Enxing et al., 2016), which uses the non-uniform sampling input-output data to build the lifted transfer function models or the lifted state-space models. Many estimation algorithms have been presented for the lifted models, e.g., a lifted transfer function model was obtained for asynchronous non-uniformly sampled- data systems in (Xie et al., 2017). (Zhou et al., 2017) presented a hierarchical recursive algorithm for asynchronous sampling Hammerstein systems by the least squares principle.

However, for Hammerstein systems with irregular updating and sampling intervals, the traditional lifted state- space models involve the problem of causality constraints, and lifted transfer function models include a larger number of parameters, resulting in increased computation complexity in the identification procedure. An input-output representation, as a novel identification model, was originally proposed for linear time-invariant processes with periodic non-uniform sampling by introducing a time-varying backward shift operator in (Xie et al., 2016). The presented model involves fewer parameters and has a more concise structure than lifted models. Following the work in (Xie et al., 2016), this paper extends the novel model to a non- uniformly sampled Hammerstein system with saturation and dead-zone, and builds an input-output identification model. Moreover, decreasing the number of estimated parameters by the key-term separation principle (Li and Ding, 2011) and replacing unmeasurable internal variables with their corresponding estimates by the auxiliary model idea (Xie and Yang, 2017), the gradient-based iterative identification algorithm is further suggested to identify the model parameters.

This paper is organized as follows. A new identification model is derived for non-uniformly sampled Hammerstein systems with saturation and dead-zone in Section 2. Section 3 provides a forgetting factor stochastic gradient algorithm and a gradient-based iterative algorithm to identify the model parameters. Section 4 offers a simulation example and a two-tank system to confirm that the gradient- based iterative algorithm proposed works effectively and performs better than the forgetting factor stochastic gradient algorithm. Last but not least, some conclusions are made in section 5.

2. THE SYSTEM DESCRIPTION AND MODEL DERIVATION

Consider the input-nonlinear systems (*i.e.*, Hammerstein systems) with non-unform sampling as shown in Fig. 1. The nonlinear part $f(\cdot)$ is followed by the linear continuous-time process P. The zero-order hold H_τ and the non-uniform sampler $S_{\tau+\Delta}$ generate non-uniformly sampled input-output data. The zero-order hold H_τ has the non-uniform updating intervals $\tau_i (i = 1,2, \dots, r.)$, producing the input $u(t)$ of $f(\cdot)$. The input data is updated r times in each frame period T, i.e., $t_0 = 0$, $t_i = \tau_1 + \tau_2 + \cdots + \tau_i$ for $i = 1,2, \dots, r$, $\mathrm{T} = \tau_1 + \tau_2 + \cdots + \tau_r$.The output $\mathrm{y}(t)$ of P is sampled by the non-uniform sampler $S_{\tau+\Delta}$, generating an output sequence $\mathrm{y}(kT + t_i + d_i)(0 \le d_i < \tau_{i+1}$ for $i = 0,1,2, \dots, r-1.)$ where d_i denotes the time lag compared with the input sampling instants. When $d_i = 0$, the systems turn into synchronous ones. Assuming that the sampling intervals $\{\tau_1, \tau_2, \cdots, \tau_r; d_0, d_1, \cdots, d_{r-1}\}$ are known, the corresponding input and output data can be known.To simplify expression, introduce the following notations: $u_i(k) \coloneqq u(kT + t_i), \overline{u}_i(k) \coloneqq \overline{u}(kT + t_i), y_{i+\Delta}(k) \coloneqq y(kT + t_i + d_i)$, where the symbol "$A \coloneqq B$" denotes that "$B$" is marked as "$A$".With the non-uniform zero-order hold $H_\tau, u(t)$ and $\overline{u}(t)$ can be described as $u(t) = u(kT + t_i) = u_i(k)$, $\overline{u}(t) = \overline{u}(kT + t_i) = \overline{u}_i(k), t \in (kT + t_i, kT + t_{i+1})$.

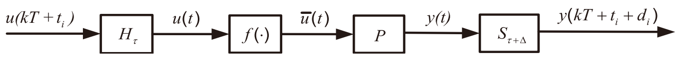

Figure 1. The schematic of non-uniformly sampled Hammerstein systems

The nonlinear block $f(\cdot)$ in Fig. 2 includes a saturation and dead-zone (Chen et al., 2012), which have the following expression,

$$\overline{u}(t) = \begin{cases} m_1(r_2 - r_1), & r_2 \le u(t), \\ m_1[u(t) - r_1], & r_1 < u(t) < r_2, \\ 0, & l_1 \le u(t) \le r_1, \\ m_2[u(t) - l_1], & l_2 < u(t) < l_1, \\ m_2(l_2 - l_1), & u(t) \le l_2, \end{cases} \tag{1}$$

where m_1 and m_2 $(m_1, m_2 > 0)$, r_1 and l_1, r_2 and l_2 $(r_2 > r_1, l_2 < l_1)$ denote the corresponding segment slopes, dead-zone points and saturation points, respectively.

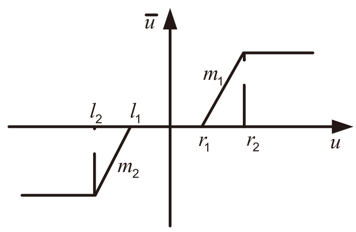

Figure 2. The saturation and dead-zone nonlinearities

To transform the piecewise expression into an analytic function, define a switching function

$$h(t) = h[u(t)] = \begin{cases} 0, & \text{if } u(t) > 0, \\ 1, & \text{if } u(t) \le 0. \end{cases}$$

Substituting it into (1), $\overline{u}(t)$ at the sampling instant $kT + t_i$ can be rewritten as

$$\begin{aligned} \overline{u}_i(k) = & m_1(r_2 - r_1)h[r_2 - u_i(k)] + m_2(l_2 - l_1)h[u_i(k) - l_2] \\ & + m_1 h[r_1 - u_i(k)]h[u_i(k) - r_2]u_i(k) \\ & - m_1 r_1 h[r_1 - u_i(k)]h[u_i(k) - r_2] \\ & + m_2 h[l_2 - u_i(k)]h[u_i(k) - l_1]u_i(k) \\ & - m_2 l_1 h[l_2 - u_i(k)]h[u_i(k) - l_1]. \end{aligned} \tag{2}$$

Suppose that the linear part P can be depicted by the following state space representation:

$$\begin{cases}\dot{\boldsymbol{x}}(t)=\boldsymbol{A}\boldsymbol{x}(t)+\boldsymbol{B}\bar{u}(t),\\ y(t)=\boldsymbol{C}\boldsymbol{x}(t)+D\bar{u}(t),\end{cases} \tag{3}$$

where $\boldsymbol{A},\boldsymbol{B},\boldsymbol{C},$ and D are constant matrices with appropriate dimensions, $\boldsymbol{x}(t)\in\mathbb{R}^n$ is the state vector, $\bar{u}(t)$ and $y(t)$ are the continuous-time process input and output, respectively.

Recent study showed that for a class of non-uniformly sampled linear systems with the state space representation, the output $y_{i+\Delta}(k)$ at the non-uniform sampling time $kT+t_i+d_i$ can be fully described with its previous $n+1$ non-uniformly updated inputs $u_i(k),u_{i-1}(k-1),\dots,u_{i-n}(k-n)$ and n non-uniform sampling outputs $y_{i-1+\Delta}(k-1),y_{i-2+\Delta}(k-2),\dots,y_{i-n+\Delta}(k-n)$ (Xie et al., 2016). Extending this novel idea to deal with the Hammer- stein system with non-uniform sampling intervals in Fig. 1, the linear block represented by the state space model can be converted to the following input-output representation,

$$\begin{aligned}y_{i+\Delta}(k)=&-a_{i,1}y_{i-1+\Delta}(k)-a_{i,2}y_{i-2+\Delta}(k)-\cdots-\\&a_{i,n}y_{i-n+\Delta}(k)+b_{i,0}\bar{u}_i(k)+b_{i,1}\bar{u}_{i-1}(k)+\cdots+\\&b_{i,n}\bar{u}_{i-n}(k),\end{aligned} \tag{4}$$

Where $a_{i,j}$ and $b_{i,j}(i=0,2,\dots,r-1;j=1,2,\dots,n)$ only depend on the coefficient matrices of the state space model, *i.e.*, $\boldsymbol{A},\boldsymbol{B},\boldsymbol{C},$ and D (Xie et al., 2016).

Notably, all the parameters b_i are combined with $\bar{u}_{i-j}(k)$, so any pair of $\alpha\bar{u}_{i-j}(k)$ and $b_{i,j}/\alpha$ will produce the same output for the model in (4) if α is a nonzero constant. In order to normalize system parameters for identification, let the first coefficient of the key-term $\bar{u}_i(k)$ be 1, *i.e.*, $b_{i,0}=1$. Then, substituting $\bar{u}_i(k)$ in (2) into (4) yields,

$$\begin{aligned}y_{i+\Delta}(k)=&m_1(r_2-r_1)h[r_2-u_i(k)]+\\&m_2(l_2-l_1)h[u_i(k)-l_2]+\\&m_1h[r_1-u_i(k)]h[u_i(k)-r_2]u_i(k)-\\&m_1r_1h[r_1-u_i(k)]h[u_i(k)-r_2]+\\&m_2h[l_2-u_i(k)]h[u_i(k)-l_1]u_i(k)-\\&m_2l_1h[l_2-u_i(k)]h[u_i(k)-l_1]-a_{i,1}y_{i-1+\Delta}(k)-\\&a_{i,2}y_{i-2+\Delta}(k)-\cdots-a_{i,n}y_{i-n+\Delta}(k)+\\&b_{i,1}\bar{u}_{i-1}(k)+\cdots+b_{i,n}\bar{u}_{i-n}(k).\end{aligned} \tag{5}$$

The information vector $\boldsymbol{\varphi}_i(k)$ and parameter vector $\boldsymbol{\theta}_i(k)$ are defined as

$$\begin{aligned}\boldsymbol{\varphi}_i(k):=\ &[h[r_2-u_i(k)],h[u_i(k)-l_2],\\&h[r_1-u_i(k)]h[u_i(k)-r_2]u_i(k),\\&-h[r_1-u_i(k)]h[u_i(k)-r_2],\\&h[l_2-u_i(k)]h[u_i(k)-l_1]u_i(k),\\&-h[l_2-u_i(k)]h[u_i(k)-l_1],-y_{i-1+\Delta}(k),\\&-y_{i-2+\Delta}(k),\dots,-y_{i-n+\Delta}(k),\bar{u}_{i-1}(k),\\&\bar{u}_{i-2}(k),\dots,\bar{u}_{i-n}(k)]^{\mathrm{T}}\in\mathbb{R}^{2n+6},\end{aligned} \tag{6}$$

$$\begin{aligned}\boldsymbol{\theta}_i:=\ &[m_1(r_2-r_1),\ m_2(l_2-l_1),\ m_1,\ m_1r_1,\ m_2,\ m_2l_1,\\&a_{i,1},\ a_{i,2},\ \dots,\ a_{i,n},\ b_{i,1},\ b_{i,2},\ \dots,\ b_{i,n}]^{\mathrm{T}}\in\mathbb{R}^{2n+6}.\end{aligned} \tag{7}$$

From (5), the system with the white noise $v_{i+\Delta}(k)$ can be denoted in matrix form

$$y_{i+\Delta}(k)=\boldsymbol{\varphi}_i^{\mathrm{T}}(k)\boldsymbol{\theta}_i(k)+v_{i+\Delta}(k). \tag{8}$$

3. THE IDENTIFICATION ALGORITHMS

In the first subsection, referring to the stochastic gradient algorithm proposed for non-uniformly sampled Hammer-stein systems in (Enxing et al., 2016), a forgetting factor stochastic gradient algorithm is presented for above model to improve the convergence rate. To make better use of system data and achieve higher estimation accuracy, the second subsection will develop a gradient-based iterative identification algorithm to identify the considered system.

3.1 The auxiliary model-based forgetting factor stochastic gradient identification algorithm

A criterion function is defined as

$$J_1(\boldsymbol{\theta}_i):=[y_{i+\Delta}(k)-\boldsymbol{\varphi}_i^{\mathrm{T}}(k)\boldsymbol{\theta}_i(k)]^2,$$

minimizing it and a stochastic gradient (SG) algorithm is derived:

$$\hat{\boldsymbol{\theta}}_i(k)=\hat{\boldsymbol{\theta}}_i(k-1)+\frac{\boldsymbol{\varphi}_i(k)}{R(k)}[y_{i+\Delta}(k)-\boldsymbol{\varphi}_i^{\mathrm{T}}(k)\hat{\boldsymbol{\theta}}_i(k-1)], \tag{9}$$

$$R(k)=R(k-1)+\|\boldsymbol{\varphi}_i(k)\|^2,\ R(0)=1. \tag{10}$$

Because of the unknown items $\bar{u}_{i-j}(k)$ and m_1, m_2, r_1, r_2, l_1, l_2 in the information vector $\boldsymbol{\varphi}_i(k)$, the SG algorithm in (9)-(10) fails to identify the parameter vector $\boldsymbol{\theta}_i$.
To solve this problem, replacing the immeasurable items with their previous estimates based on the auxiliary model identification idea, yields

$$\begin{aligned}\hat{\boldsymbol{\varphi}}_i(k)=\ &[h[\hat{r}_2(k-1)-u_i(k)],\ h[u_i(k)-\hat{l}_2(k-1)],\\&h[\hat{r}_1(k-1)-u_i(k)]h[u_i(k)-\hat{r}_2(k-1)]u_i(k),\\&-h[\hat{r}_1(k-1)-u_i(k)]h[u_i(k)-\hat{r}_2(k-1)],\\&h[\hat{l}_2(k-1)-u_i(k)]h[u_i(k)-\hat{l}_1(k-1)]u_i(k),\\&h[\hat{l}_2(k-1)-u_i(k)]h[u_i(k)-\hat{l}_1(k-1)],\\&-y_{i-1+\Delta}(k),\ -y_{i-2+\Delta}(k),\ \dots,\ -y_{i-n+\Delta}(k),\\&\hat{\bar{u}}_{i-1}(k-1),\hat{\bar{u}}_{i-2}(k-1),\ \dots,\hat{\bar{u}}_{i-n}(k-1)]^{\mathrm{T}}\in\mathbb{R}^{2n+6}.\end{aligned}$$

Replacing unknown m_1, m_2, r_1, r_2, l_1 and l_2 with their estimates in (2), the estimate of $\bar{u}_i(k)$ can be calculated by

$$\begin{aligned}\hat{\bar{u}}_i(k)=\ &\hat{m}_1(k)[\hat{r}_2(k)-\hat{r}_1(k)]h[\hat{r}_2(k)-u_i(k)]+\\&\hat{m}_2(k)[\hat{l}_2(k)-\hat{l}_1(k)]h[u_i(k)-\hat{l}_2(k)]+\\&\hat{m}_1(k)h[\hat{r}_1(k)-u_i(k)]h[u_i(k)-\hat{r}_2(k)]u_i(k)-\\&\hat{m}_1(k)\hat{r}_1(k)h[\hat{r}_1(k)-u_i(k)]h[u_i(k)-\hat{r}_2(k)]+\\&\hat{m}_2(k)h[\hat{l}_2(k)-u_i(k)]h[u_i(k)-\hat{l}_1(k)]u_i(k)-\\&\hat{m}_2(k)\hat{l}_1(k)h[\hat{l}_2(k)-u_i(k)]h[u_i(k)-\hat{l}_1(k)].\end{aligned}$$

To increase the convergence rate, a parameter λ called the forgetting factor is introduced into the SG algorithm. Therefore, the forgetting factor gradient algorithm based on the auxiliary model (AM-FG) for estimating the parameters θ_i is deduced as:

$$\widehat{\boldsymbol{\theta}}_i(k) = \widehat{\boldsymbol{\theta}}_i(k-1) + \frac{\widehat{\boldsymbol{\varphi}}_i(k)}{R(k)}\left[y_{i+\Delta}(k) - \widehat{\boldsymbol{\varphi}}_i^{\mathrm{T}}(k)\widehat{\boldsymbol{\theta}}_i(k-1)\right], \quad (11)$$

$$R(k) = \lambda R(k-1) + \|\widehat{\boldsymbol{\varphi}}_i(k)\|^2,\ 0 \le \lambda \le 1,\ R(0) = 1, \quad (12)$$

$$\begin{aligned}\widehat{\boldsymbol{\theta}}_i(k) =& [\widehat{m}_1(k)[\hat{r}_2(k) - \hat{r}_1(k)], \widehat{m}_2(k)[\hat{l}_2(k) - \hat{l}_1(k)],\\ & \widehat{m}_1(k), \widehat{m}_1(k)\hat{r}_1(k), \widehat{m}_2(k), \widehat{m}_2(k)\hat{l}_1(k), \hat{a}_{i,1}(k),\\ & \hat{a}_{i,2}(k), \dots, \hat{a}_{i,n}(k), \hat{b}_{i,1}(k), \hat{b}_{i,2}(k), \dots, \hat{b}_{i,n}(k)]^{\mathrm{T}}, \end{aligned} \quad (13)$$

$$\widehat{m}_1(k) = \widehat{\boldsymbol{\theta}}_i(k)(3),\ \widehat{m}_2(k) = \widehat{\boldsymbol{\theta}}_i(k)(5), \quad (14)$$

$$\hat{r}_1(k) = \frac{\widehat{\boldsymbol{\theta}}_i(k)(4)}{\widehat{m}_1(k)},\ \hat{r}_2(k) = \frac{\widehat{\boldsymbol{\theta}}_i(k)(1)}{\widehat{m}_1(k)} + \hat{r}_1(k), \quad (15)$$

$$\hat{l}_1(k) = \frac{\widehat{\boldsymbol{\theta}}_i(k)(6)}{\widehat{m}_2(k)},\ \hat{l}_2(k) = \frac{\widehat{\boldsymbol{\theta}}_i(k)(2)}{\widehat{m}_2(k)} + \hat{l}_1(k), \quad (16)$$

$$\begin{aligned}\widehat{\boldsymbol{\varphi}}_i(k) =& [h[\hat{r}_2(k-1) - u_i(k)],\ h[u_i(k) - \hat{l}_2(k-1)],\\ & h[\hat{r}_1(k-1) - u_i(k)]h[u_i(k) - \hat{r}_2(k-1)]u_i(k),\\ & -h[\hat{r}_1(k-1) - u_i(k)]h[u_i(k) - \hat{r}_2(k-1)],\\ & h[\hat{l}_2(k-1) - u_i(k)]h[u_i(k) - \hat{l}_1(k-1)]u_i(k),\\ & h[\hat{l}_2(k-1) - u_i(k)]h[u_i(k) - \hat{l}_1(k-1)],\\ & -y_{i-1+\Delta}(k),\ -y_{i-2+\Delta}(k),\ \dots,\ -y_{i-n+\Delta}(k),\\ & \hat{\bar{u}}_{i-1}(k-1), \hat{\bar{u}}_{i-2}(k-1),\ \dots, \hat{\bar{u}}_{i-n}(k-1)]^{\mathrm{T}}, \end{aligned} \quad (17)$$

$$\begin{aligned}\hat{\bar{u}}_i(k) =& \widehat{m}_1(k)[\hat{r}_2(k) - \hat{r}_1(k)]h[\hat{r}_2(k) - u_i(k)] +\\ & \widehat{m}_2(k)[\hat{l}_2(k) - \hat{l}_1(k)]h[u_i(k) - \hat{l}_2(k)] +\\ & \widehat{m}_1(k)h[\hat{r}_1(k) - u_i(k)]h[u_i(k) - \hat{r}_2(k)]u_i(k) -\\ & \widehat{m}_1(k)\hat{r}_1(k)h[\hat{r}_1(k) - u_i(k)]h[u_i(k) - \hat{r}_2(k)] +\\ & \widehat{m}_2(k)h[\hat{l}_2(k) - u_i(k)]h[u_i(k) - \hat{l}_1(k)]u_i(k) -\\ & \widehat{m}_2(k)\hat{l}_1(k)h[\hat{l}_2(k) - u_i(k)]h[u_i(k) - \hat{l}_1(k)]. \end{aligned} \quad (18)$$

where $\widehat{\boldsymbol{\theta}}_i(k)(j)$ denotes the jth element of parameter vector $\widehat{\boldsymbol{\theta}}_i(k)$.
Then the identification steps of the AM-FG algorithm in (11)-(18) are summarized as:

Step 1: To initialize: let $k = 1$, set the data length L, and the Initial Values: $\boldsymbol{\theta}_i(0) = \mathbf{1}_{2n+6}/p_0$ ($\mathbf{1}_{2n+6}$ stands for an $2n + 6$-dimensional column vector whose elements are 1.), $p_0 = 10^6$, $\hat{\bar{u}}_i(0) = 1/p_0$, $R(0) = 1$.

Step 2: Collect the input and output data $\{u_i(k),\ y_{i+\Delta}(k)\}$, then form the information vector $\widehat{\boldsymbol{\varphi}}_i(k)$ by (17).

Step 3: Choose the value of λ and calculate the value of $R(k)$ by (12), then update the parameter vector $\widehat{\boldsymbol{\theta}}_i(k)$ by (11).

Step 4: Compute the parameters $\widehat{m}_1(k)$, $\widehat{m}_2(k)$, $\hat{r}_1(k)$, $\hat{r}_2(k)$, $\hat{l}_1(k)$, $\hat{l}_2(k)$ by (13)-(16), then calculate auxiliary model output $\hat{\bar{u}}_i(k)$ using (18).

Step 5: If $k = L$, terminate the procedure; or else, let $k = k + 1$ and transfer to Step 2.

3.2 The gradient based iterative identification algorithm

This section gives a gradient-based iterative algorithm for identifying the model in (8) by introducing the negative gradient search principle. And the immeasurable variables in the information vector are dealt with the auxiliary model.

Firstly, the stacked output vector $\boldsymbol{Y}(L)$, stacked information matrix $\boldsymbol{\Phi}(L)$ and white noise vector $\boldsymbol{V}(L)$ are defined as follows:

$$\begin{aligned}\boldsymbol{Y}_{i+\Delta}(L) &= \begin{bmatrix} y_{i+\Delta}(L) \\ y_{i+\Delta}(L-1) \\ \vdots \\ y_{i+\Delta}(1) \end{bmatrix} \in \mathbb{R}^L,\\ \boldsymbol{\Phi}_i(L) &= \begin{bmatrix} \boldsymbol{\varphi}_i^{\mathrm{T}}(L) \\ \boldsymbol{\varphi}_i^{\mathrm{T}}(L-1) \\ \vdots\ \boldsymbol{\varphi}_i^{\mathrm{T}}(1) \end{bmatrix} \in \mathbb{R}^{L\times n},\\ \boldsymbol{V}_{i+\Delta}(L) &= \begin{bmatrix} v_{i+\Delta}(L) \\ v_{i+\Delta}(L-1) \\ \vdots \\ v_{i+\Delta}(1) \end{bmatrix} \in \mathbb{R}^L, \end{aligned} \quad (19)$$

where L means the data length. Equation (8) can be described by the matrix form:

$$\boldsymbol{Y}_{i+\Delta}(L) = \boldsymbol{\Phi}_i(L)\boldsymbol{\theta}_i + \boldsymbol{V}_{i+\Delta}(L).$$

Define the criterion function:

$$J_2(\boldsymbol{\theta}_i) := \tfrac{1}{2}\|\boldsymbol{Y}_{i+\Delta}(L) - \boldsymbol{\Phi}_i(L)\boldsymbol{\theta}_i\|^2 \quad (20)$$

Taking the gradient of $J_2(\boldsymbol{\theta}_i)$ with respect to $\boldsymbol{\theta}_i$ yields

$$\mathrm{grad}[J_2(\boldsymbol{\theta}_i)] = \frac{\partial J_2(\boldsymbol{\theta}_i)}{\partial \boldsymbol{\theta}_i} = -[\boldsymbol{\Phi}_i(L)]^{\mathrm{T}}[\boldsymbol{Y}_{i+\Delta}(L) - \boldsymbol{\Phi}_i(L)\boldsymbol{\theta}_i].$$

Minimizing the criterion function in (20) by the negative gradient search principle, the gradient-based iterative algorithm is derived:

$$\begin{aligned}\widehat{\boldsymbol{\theta}}_i^p &= \widehat{\boldsymbol{\theta}}_i^{p-1} - \mu_p \mathrm{grad}\left[J_2\left(\widehat{\boldsymbol{\theta}}_i^{p-1}\right)\right]\\ &= \widehat{\boldsymbol{\theta}}_i^{p-1} + \mu_p\left[\boldsymbol{\Phi}_i^p(L)\right]^{\mathrm{T}}\left[\boldsymbol{Y}_{i+\Delta}(L) - \boldsymbol{\Phi}_i^p(L)\widehat{\boldsymbol{\theta}}_i^{p-1}\right], \end{aligned} \quad (21)$$

where $p = 1,2,3,\cdots$ and μ_p denote the iteration variable and the iterative step-size, respectively, $\widehat{\boldsymbol{\theta}}_i^p$ is the estimate of $\boldsymbol{\theta}_i$ at iteration p.

Due to the unknown item $\bar{u}_{i-j}(k)$ and unknown parameters $m_1, m_2, r_1, r_2, l_1, l_2$ in $\boldsymbol{\varphi}_i(k)$, the iterative algorithm fails to identify system parameters. Using the previous iterative estimates to replace the unknown item and unknown parameters, respectively, a gradient-based iterative identification (GI) algorithm can be deduced as

$$\hat{\boldsymbol{\theta}}_i^p = \hat{\boldsymbol{\theta}}_i^{p-1} + \mu_p [\hat{\boldsymbol{\Phi}}_i^p(L)]^{\mathrm{T}} [\boldsymbol{Y}_{i+\Delta}(L) - \hat{\boldsymbol{\Phi}}_i^p(L)\hat{\boldsymbol{\theta}}_i^{p-1}], \quad (22)$$

$$\boldsymbol{Y}_{i+\Delta}(L) = [y_{i+\Delta}(L), y_{i+\Delta}(L-1), \cdots, y_{i+\Delta}(1)]^{\mathrm{T}}, \quad (23)$$

$$\hat{\boldsymbol{\Phi}}_i^p(L) = [\hat{\boldsymbol{\varphi}}_i^p(L), \hat{\boldsymbol{\varphi}}_i^p(L-1), \cdots, \hat{\boldsymbol{\varphi}}_i^p(1)]^{\mathrm{T}}, \quad (24)$$

$$\begin{aligned}\hat{\boldsymbol{\varphi}}_i^p(k) := [&h[\hat{r}_2^{p-1} - u_i(k)], h[u_i(k) - \hat{l}_2^{p-1}],\\ &h[\hat{r}_1^{p-1} - u_i(k)]h[u_i(k) - \hat{r}_2^{p-1}]u_i(k),\\ &-h[\hat{r}_1^{p-1} - u_i(k)]h[u_i(k) - \hat{r}_2^{p-1}],\\ &h[\hat{l}_2^{p-1} - u_i(k)]h[u_i(k) - \hat{l}_1^{p-1}]u_i(k),\\ &-h[\hat{l}_2^{p-1} - u_i(k)]h[u_i(k) - \hat{l}_1^{p-1}], -y_{i-1+\Delta}(k),\\ &-y_{i-2+\Delta}(k), \cdots, -y_{i-n+\Delta}(k), \hat{\bar{u}}_{i-1}^{p-1}(k),\\ &\hat{\bar{u}}_{i-2}^{p-1}(k), \cdots, \hat{\bar{u}}_{i-n}^{p-1}(k)]^{\mathrm{T}} \in \mathbb{R}^{2n+6}, \end{aligned} \quad (25)$$

$$\begin{aligned}\hat{\bar{u}}_i^p(k) = &\hat{m}_1^p(\hat{r}_2^p - \hat{r}_1^p)h[\hat{r}_2^p - u_i(k)] +\\ &\hat{m}_2^p(\hat{l}_2^p - \hat{l}_1^p)h[u_i(k) - \hat{l}_2^p] +\\ &\hat{m}_1^p h[\hat{r}_1^p - u_i(k)]h[u_i(k) - \hat{r}_2^p]u_i(k) -\\ &\hat{m}_1^p\hat{r}_1^p h[\hat{r}_1^p - u_i(k)]h[u_i(k) - \hat{r}_2^p] +\\ &\hat{m}_2^p h[\hat{l}_2^p - u_i(k)]h[u_i(k) - \hat{l}_1^p]u_i(k) -\\ &\hat{m}_2^p\hat{l}_1^p h[\hat{l}_2^p - u_i(k)]h[u_i(k) - \hat{l}_1^p], \end{aligned} \quad (26)$$

$$\begin{aligned}\hat{\boldsymbol{\theta}}_i^p = [&\hat{m}_1^p[\hat{r}_2^p - \hat{r}_1^p], \hat{m}_2^p[\hat{l}_2^p - \hat{l}_1^p], \hat{m}_1^p, \hat{m}_1^p\hat{r}_1^p, \hat{m}_2^p,\\ &\hat{m}_2^p\hat{l}_1^p, \hat{a}_{i,1}^p, \hat{a}_{i,2}^p, \dots, \hat{a}_{i,n}^p, \hat{b}_{i,1}^p, \hat{b}_{i,2}^p, \dots, \hat{b}_{i,n}^p]^{\mathrm{T}}, \end{aligned} \quad (27)$$

$$\begin{aligned}&\hat{m}_1^p = \hat{\boldsymbol{\theta}}_i^p(3), \ \hat{m}_2^p = \hat{\boldsymbol{\theta}}_i^p(5),\\ &\hat{r}_1^p = \frac{\hat{\boldsymbol{\theta}}_i^p(4)}{\hat{m}_1^p}, \ \hat{r}_2^p = \frac{\hat{\boldsymbol{\theta}}_i^p(1)}{\hat{m}_1^p} + \hat{r}_1^p,\\ &\hat{l}_1^p = \frac{\hat{\boldsymbol{\theta}}_i^p(6)}{\hat{m}_2^p}, \ \hat{l}_2^p = \frac{\hat{\boldsymbol{\theta}}_i^p(2)}{\hat{m}_2^p} + \hat{l}_1^p, \end{aligned} \quad (28)$$

$$0 < \mu_p \leq \frac{2}{\lambda_{\max}\left\{[\hat{\boldsymbol{\Phi}}_i^p(L)]^{\mathrm{T}}\hat{\boldsymbol{\Phi}}_i^p(L)\right\}}. \quad (29)$$

The identification steps of the GI algorithm are summed up:

Step 1: To initialize: set the data length L and a small estimation precision ε_0, and let $p = 1$, $\boldsymbol{\theta}_i^0 = \mathbf{1}_{2n+6}/p_0$, $p_0 = 10^6$, $\hat{\bar{u}}_i^0(k) = 1/p_0$.

Step 2: Collect the input and output data $\{u_i(k), y_{i+\Delta}(k)\}$, then construct the stacked output vector $\boldsymbol{Y}_{i+\Delta}(L)$ by (23).

Step 3: Construct the information vector $\hat{\boldsymbol{\varphi}}_i^p(k)$ and stacked information matrix $\hat{\boldsymbol{\Phi}}_i^p(L)$ by (25) and (24), respectively.

Step 4: Select the iterative step-size μ_p by (29), then update the parameter vector $\hat{\boldsymbol{\theta}}_i^p$ by (22).

Step 5: Calculate nonlinear parameters $\hat{m}_1^p$, $\hat{m}_2^p$, $\hat{r}_1^p$, $\hat{r}_2^p$, $\hat{l}_1^p$, $\hat{l}_2^p$ by (27)-(28) and auxiliary model output $\hat{\bar{u}}_i^p(k)$ by (26), respectively.

Step 6: Compare $\hat{\boldsymbol{\theta}}_i^p$ and $\hat{\boldsymbol{\theta}}_i^{p-1}$. End the procedure and get the iterative times p until $\|\hat{\boldsymbol{\theta}}_i^p - \hat{\boldsymbol{\theta}}_i^{p-1}\| \leq \varepsilon_0$; otherwise, let $p = p + 1$ and goto Step 2.

4. EXAMPLES

In this section, a numerical Hammerstein system and a continuous two-tank system with saturation and dead-zone nonlinearity are used to show the effectiveness of the GI algorithm.

4.1 Numerical example

To demonstrate how the proposed algorithms work and make a comparison between them, this section gives a numerical example, which has a Hammerstein system as following:

$$\begin{cases}\dot{\boldsymbol{x}}(t) &= \begin{bmatrix}-0.35 & -0.045\\ 1 & 0\end{bmatrix}\boldsymbol{x}(t) + \begin{bmatrix}0.03\\ 0\end{bmatrix}\bar{u}(t),\\ y(t) &= [0, 0.035]\boldsymbol{x}(t) + 0.035\bar{u}(t).\end{cases}$$

The nonlinearity is shown in Figure 2, with

$$\begin{aligned}\boldsymbol{\omega} &= [m_1, m_2, r_1, r_2, l_1, l_2]\\ &= [0.44, 0.1, 0.04, 0.54, -0.15, -0.75].\end{aligned}$$

Assume $T = 13s$, $r = 2$, $\tau_1 = 6s$, $\tau_2 = 7s$ and $d_0 = 3.5s$, $d_1 = 4s$. The input $\{u_i(k), i = 0,1\}$ is a random signal sequence with zero mean and unit variance, while the noise $\{v_i(k), i = 0,1\}$ is white Gaussian with zero mean and constant variance $\sigma^2 = 0.2^2$. The estimation error is defined as

$$\varepsilon := \frac{\sum_{i=0}^{1}\left[||\hat{\boldsymbol{a}}_i - \boldsymbol{a}_i||^2 + ||\hat{\boldsymbol{b}}_i - \boldsymbol{b}_i||^2\right] + \|\hat{\boldsymbol{\omega}} - \boldsymbol{\omega}\|^2}{\sum_{i=0}^{1}[\|\boldsymbol{a}_i\|^2 + \|\boldsymbol{b}_i\|^2] + \|\boldsymbol{\omega}\|^2} \times 100\%. \quad (30)$$

Apply the AM-FG algorithm in (11)-(18) and the GI algorithm in (22)-(29) to identify the considered system. Taking the forgetting factors $\lambda = 0.99, 0.98, 0.97, 0.96$, respectively, the parameter estimates and their errors of the AM-FG algorithm are shown in Table 1, and the corresponding errors are plotted in Fig. 3. With the data length $L = 5000$, the estimates and errors of the GI algorithm are shown in Table 2, and the corresponding estimation error ε versus iteration variable p is plotted in Fig. 4. Fig. 5 shows the mean estimation error of the GI algorithm with different random sequences.

Table 1. The numerical example: estimates and errors of the AM-FG algorithm (L = 5000)

k	$\lambda = 0.99$	$\lambda = 0.98$	$\lambda = 0.97$	$\lambda = 0.96$	True values
$a_{0,1}$	-0.23805	-0.27083	-0.26446	-0.24632	-0.26456
$a_{0,2}$	0.03494	0.05586	0.03051	0.05072	0.04400
$b_{0,1}$	0.04465	0.02712	0.00729	-0.02672	0.03926
$b_{0,2}$	-0.05310	-0.12406	-0.00987	-0.04262	0.00388
$a_{1,1}$	-0.13800	-0.16666	-0.14049	-0.14027	-0.15513
$a_{1,2}$	0.04337	0.05758	0.04807	0.05501	0.04564
$b_{1,1}$	0.04161	0.02526	0.00663	-0.02974	0.04229
$b_{1,2}$	-0.06437	-0.13337	-0.03266	-0.04888	0.00642
m_1	0.23007	0.25997	0.23385	0.23992	0.44000
m_2	0.00034	0.00090	0.06945	0.05572	0.10000
r_1	-0.01828	0.05859	0.07934	0.13975	0.04000
r_2	0.94251	0.98636	1.09590	1.24970	0.54000

k	$\lambda = 0.99$	$\lambda = 0.98$	$\lambda = 0.97$	$\lambda = 0.96$	True values
l_1	-10.79600	-3.09350	-0.70776	-1.99450	-0.15000
l_2	-7.24000	-7.89460	-1.61710	-2.84570	-0.75000
$\varepsilon(\%)$	6.77240	8.27360	4.93360	6.92360	

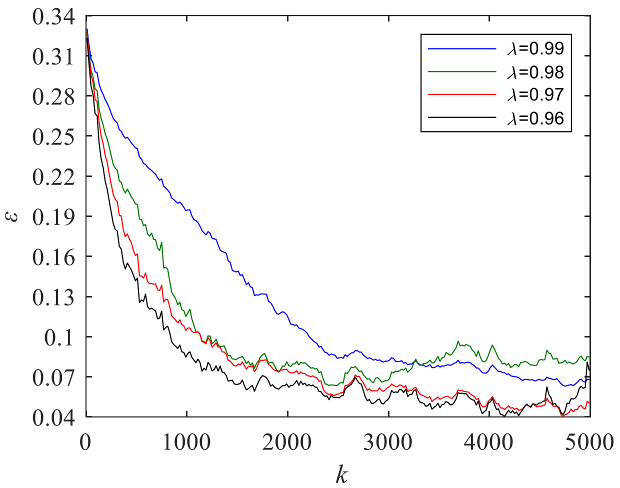

Figure 3. The numerical example: parameter estimation error of the AM-FG algorithm ε vs. k

Table 2. The numerical example: estimates and errors of the GI algorithm

k	50	100	200	400	600	800	True values
$a_{0,1}$	-0.25722	-0.25622	-0.25360	-0.25250	-0.25273	-0.25275	-0.26456
$a_{0,2}$	0.02137	0.02765	0.02867	0.02981	0.03010	0.03009	0.04400
$b_{0,1}$	0.02179	0.03433	0.04629	0.04301	0.04235	0.04226	0.03926
$b_{0,2}$	-0.01425	-0.00577	0.00320	0.00326	0.00399	0.00395	0.00388
$a_{1,1}$	-0.15359	-0.14860	-0.14459	-0.14317	-0.14338	-0.14342	-0.15513
$a_{1,2}$	0.02544	0.02989	0.03098	0.03207	0.03237	0.03234	0.04564
$b_{1,1}$	0.01568	0.03265	0.04838	0.04599	0.04539	0.04534	0.04229
$b_{1,2}$	-0.01056	-0.00298	0.00530	0.00518	0.00597	0.00597	0.00642
m_1	0.21961	0.25750	0.32139	0.41632	0.44026	0.44034	0.44000
m_2	0.04157	0.04202	0.04561	0.08411	0.08400	0.08395	0.10000
r_1	-0.25733	-0.16011	-0.04062	0.05526	0.06791	0.06833	0.04000
r_2	0.73432	0.68232	0.63034	0.57481	0.55872	0.55911	0.54000
l_1	0.57935	0.49485	0.37891	-0.09063	-0.09397	-0.09642	-0.15000
l_2	-1.02560	-1.13220	-1.13200	-0.91626	-0.92013	-0.92316	-0.75000
$\varepsilon(\%)$	6.16620	4.24160	1.98760	0.17035	0.12281	0.12301	

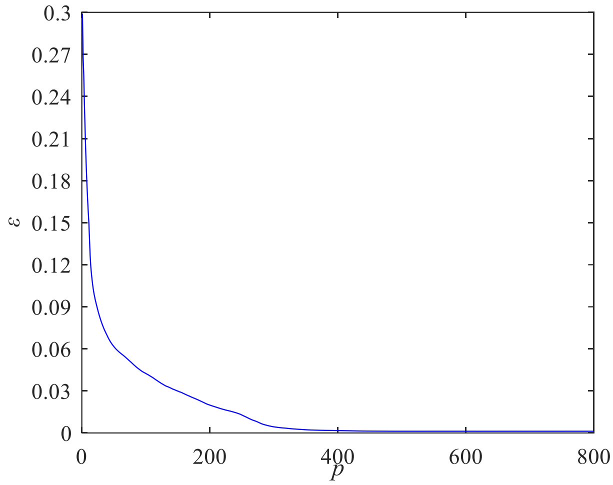

Figure 4. The numerical example: parameter estimation error of the GI algorithm ε vs. p

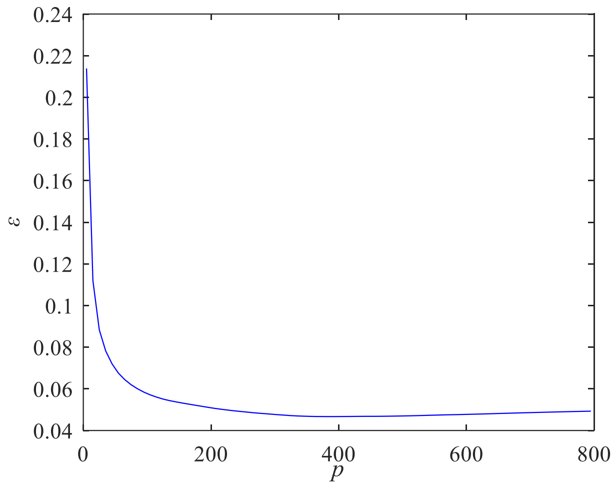

Figure 5. The numerical example: mean estimation error of the GI algorithm ε vs. p

From Table 1 and Fig. 3, it is apparent that for the AM-FG algorithm, its estimation error decreases as the forgetting factor λ decreases. However, some parameter estimates deviate far from the true ones. And the parameter estimates also fluctuate a lot when λ is smaller than 0.97. The results illustrate that the effectiveness of the AM- FG algorithm for this considered non-uniform sampling Hammerstein system needs to be further improved.

For the GI algorithm, it's evident that its estimation error becomes smaller and all estimates gradually approach to their true values with the increase of iterations p, and its convergence rate is very speedy from table 2 and Fig. 4.

Comparing Table 1 with Table 2, the estimates of the GI algorithm are much closer to the true values than that of the AM-FG algorithm, and have significantly smaller parameter estimation errors in the last rows in these Tables. The results validate that the proposed gradient- based iterative identification method has a more superior estimation accuracy.

Moreover, changing the random sequences (8:130), Fig. 5 depicts that the mean estimation errors are fast and smooth close to the true values, which further illustrates that the GI algorithm has a smooth and good performance.

4.2 Two-tank system

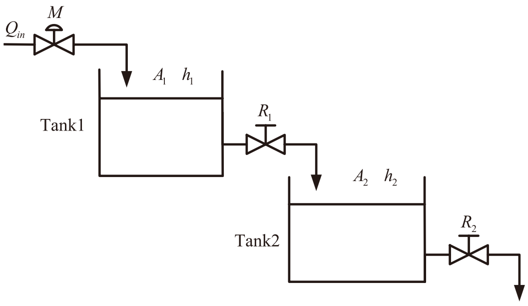

Figure 6. Schematic diagram of two-tank system

A two-tank system in Fig. 6 is used as a practical process example. The motorized valve M may include a saturation and dead-zone characteristic, which has translation relation with that of Fig. 2. The output of the valve is zero when its input signal is not big enough to open the valve. The output of the valve may remain constant when its input changes in a small range. The insensitive phenomenon may be caused by some actuator arrearage faults and a PID control algorithm with insensitive region aimed at avoiding damage from frequent action of the actuator. Therefore, the two-tank system can be tailored as a non- uniform sampling process for system identification and algorithm testing. In a simplified and linearized model, the two-tank system is modeled as

$$A_1 \frac{dh_1}{dt} = Q_{in} - c_1 h_1,$$
$$A_2 \frac{dh_2}{dt} = c_1 h_1 - c_2 h_2,$$

where Q_{in} is the input flow rate; $A_1 = 1$ and $A_2 = 1.2$ are the cross-section areas of the two tanks respectively; $c1 = 0.5$ and $c2 = 0.8$ the coefficients after linearization and associated with the valves R_1 and R_2 respectively; h_1 and h_2 the liquid levels in Tank1 and Tank2 respectively.

The nonlinearity parameters are set as $[m_1, m_2, r_1, r_2, l_1, l_2] = [0.38, 0.02, 0.8, 2.6, 0.65, 0.02]$ the sample time selected as $T = 5s$, $r = 2$, $\tau_1 = 3s$, $\tau_2 = 2s$ and $d_0 = 2.5s$, $d_1 = 1.5s$. Through the simulation of these two algorithms, the estimation errors of the GI algorithm and AM-FG algorithm are 0.23365% and 7.67490%, respectively. The estimation errors of the GI algorithm are plotted in Fig. 7. It reveals that the estimation error converges quickly and smoothly. The results verify that the GI algorithm can well identify all model parameters with high accuracy.

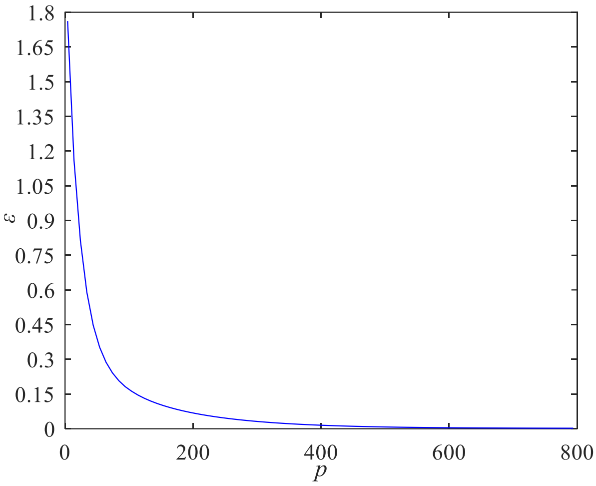

Figure 7. The two-tank system: the estimation error of the GI algorithm ε vs. p

5. CONCLUSIONS

By introducing the input-output expression of the n-order difference equation to describe the linear block with state space representation, a concise identification model is first established for a non-uniformly sampled Hammerstein system with saturation and dead zone. A gradient-based iterative (GI) algorithm is derived to identify model parameters effectively. By analyzing simulation results including a numerical example and a two-tank system, the GI algorithm has better identification performance on its superior estimation accuracy than the forgetting factor gradient algorithm based on the auxiliary model (AM-FG) algorithm. The proposed approach is applicable to tackling Hammerstein systems with other types of nonlinear blocks. It also provides a new insight for further research on parameter identification of non-uniformly sampled systems with more complex nonlinearities.

REFERENCES

Amer, Y., El-Sayed, A., and Ahmed, E. (2021). On controlling the nonlinear vibrations of a rectangular thin plate with time delay feedback. *Control Engineering and Applied Informatics*, 23, 40–52.

Atitallah, A., Bedoui, S., and Abderrahim, K. (2020). Joint parameter and time-delay identification algorithm and its convergence analysis for wiener time-delay systems. *Circuits, Systems, and Signal Processing*, 39(1), 199–222.

Avila, F.R., Duarte, L.T., and Biscainho, L.W. (2017). On the sparsity-based identification and compensation of hammerstein systems. *IEEE Signal Processing Letters*, 24(9), 1363–1367.

Chen, J., Wang, X., and Ding, R. (2012). Gradient based estimation algorithm for hammerstein systems with saturation and dead-zone nonlinearities. *Applied Mathematical Modelling*, 36(1), 238–243.

Ding, F. (2013). Hierarchical multi-innovation stochastic gradient algorithm for hammerstein nonlinear system modeling. *Applied Mathematical Modelling*, 37(4), 1694–1704.

Ding, F., Liu, X., and Chu, J. (2013). Gradient-based and least-squares-based iterative algorithms for hammerstein systems using the hierarchical identification principle. *IET Control Theory & Applications*, 7(2), 176–184.

Ding, F., Qiu, L., and Chen, T. (2009). Reconstruction of continuous-time systems from their non-uniformly sampled discrete-time systems. *Automatica*, 45(2), 324–332.

Ding, J. and Lin, J. (2014). Modified subspace identification for periodically non-uniformly sampled systems by using the lifting technique. *Circuits, Systems, and Signal Processing*, 33(5), 1439–1449.

Dong, Z. (2015). Model-free power-level control of mhtgrs against input saturation and dead-zone. *IEEE Transactions on Nuclear Science*, 62(6), 3297–3310.

Enxing, Z., Ranran, L., Yifeng, J., Yuxia, S., and FuYin, N. (2016). Stochastic gradient identification for hammerstein systems with non-uniformly sampling. *Computer Systems Science and Engineering*, 31(6), 439–444.

Gao, X., Ren, X., Zhu, C., and Zhang, C. (2015). Identification and control for hammerstein systems with hysteresis non-linearity. *IET Control Theory & Applications*, 9(13), 1935–1947.

Giri, F., Rochdi, Y., Brouri, A., and Chaoui, F.Z. (2011). Parameter identification of hammerstein systems containing backlash operators with arbitrary-shape parametric borders. *Automatica*, 47(8), 1827–1833.

Hu, Q., Ma, G., and Xie, L. (2008). Robust and adaptive variable structure output feedback control of uncertain systems with input nonlinearity. *Automatica*, 44(2), 552–559.

Li, J. and Ding, F. (2011). Maximum likelihood stochastic gradient estimation for hammerstein systems with colored noise based on the key term separation technique. *Computers & Mathematics with Applications*, 62(11), 4170–4177.

Liu, Y., Ding, F., and Shi, Y. (2012). Least squares estimation for a class of non-uniformly sampled systems based on the hierarchical identification principle. *Circuits, Systems, and Signal Processing*, 31(6), 1985–2000.

Liu, Y. and Bai, E.W. (2007). Iterative identification of hammerstein systems. *Automatica*, 43(2), 346–354.

Na, J., Herrmann, G., and Zhang, K. (2017). Improving transient performance of adaptive control via a modified reference model and novel adaptation. *International Journal of Robust and Nonlinear Control*, 27(8), 1351– 1372.

Oh, S.Y. and Park, D.J. (2000). Design of novel two-layered fuzzy logic controller for plants with time-varying dead-zone and saturation characteristics. *Journal of Intelligent & Fuzzy Systems,* 8(3), 173–190.

Paduart, J., Lauwers, L., Pintelon, R., and Schoukens, J. (2012). Identification of a wiener–hammerstein system using the polynomial nonlinear state space approach. *Control Engineering Practice*, 20(11), 1133–1139.

Pan, J., Li, W., and Zhang, H. (2018). Control algorithms of magnetic suspension systems based on the improved double exponential reaching law of sliding mode control. *International Journal of Control, Automation and Systems*, 16(6), 2878–2887.

Pu, Y., Yang, Y., and Chen, J. (2021). Some stochastic gradient algorithms for hammerstein systems with piece- wise linearity. *Circuits, Systems, and Signal Processing*, 40(4), 1635–1651.

Schoukens, M. and Tiels, K. (2017). Identification of block-oriented nonlinear systems starting from linear approximations: A survey. *Automatica*, 85, 272–292.

Tahoun, A. (2017). A new online delay estimation-based robust adaptive stabilizer for multi-input neutral systems with unknown actuator nonlinearities. *ISA transactions*, 70, 139–148.

Xia, G., Shao, X., Zhao, A., and Wu, H. (2013). Adaptive neural network control with backstepping for surface ships with input dead-zone. *Mathematical Problems in Engineering*, 2013.

Xie, L. and Yang, H. (2017). Auxiliary model based multi-innovation stochastic gradient identification algorithm for periodically non-uniformly sampled-data hammerstein systems. *algorithms*, 10(3), 84.

Xie, L., Yang, H., and Ding, F. (2017). Identification of non-uniformly sampled-data systems with asynchronous input and output data. *Journal of the Franklin Institute*, 354(4), 1974–1991.

Xie, L., Yang, H., Ding, F., and Huang, B. (2016). Novel model of non-uniformly sampled-data systems based on a time-varying backward shift operator. *Journal of Process Control*, 43, 38–52.

Xing, L., Wen, C., Su, H., Cai, J., and Wang, L. (2015). A new adaptive control scheme for uncertain nonlinear systems with quantized input signal. *Journal of the Franklin Institute*, 352(12), 5599–5610.

Xu, L. (2017). The parameter estimation algorithms based on the dynamical response measurement data. *Advances in Mechanical Engineering*, 9(11), 1687814017730003.

Xu, L., Xiong, W., Alsaedi, A., and Hayat, T. (2018). Hierarchical parameter estimation for the frequency response based on the dynamical window data. *International Journal of Control, Automation and Systems*, 16(4), 1756–1764.

Zhang, J., Yu, F., and Chin, K. (2017). Recursive identification of hammerstein systems with dead-zone nonlinearity in the presence of bounded noise. *International Journal of Systems Science*, 48(11), 2394–2404.

Zhou, L., Li, X., Shan, L., Xia, J., and Chen, W. (2017). Hierarchical recursive least squares parameter estimation of non-uniformly sampled hammerstein nonlinear systems based on kalman filter. *Journal of the Franklin Institute*, 354(10), 4231–4246.